Solar System Dynamics

Chris Williams
Student 1607421
HET 602 Project

28th November 2001

Introduction

In the early 17th century Johannes Kepler (1571-1630), working with his predecessor, Tycho Brahe's, detailed record of planetary positions, determined three basic laws that elegantly encapsulated the motion of the planets:

- Each planet orbits the Sun on an elliptical path with the Sun at one focus.
- An imaginary line connecting a planet to the Sun sweeps out equal areas in equal times.
- The time (T) a planet takes to orbit the Sun squared is proportional to the average distance from the Sun cubed. Geometry dictates that the average distance is equal to half the long axis or, semi-major axis (a), of the ellipse. Expressed in symbolic form: $T^2 \propto a^3$

Kepler's empirical derivation described planetary celestial wanderings very well but shed little light the underlying principle that should cause the planets to follow such paths.

Later in the century, Sir Isaac Newton (1642-1727) had an insight that was destined to revolutionise celestial mechanics. Newton realised that if the force that made objects fall to ground, now called gravity, extended all the way to the Moon it could keep the Moon orbiting the Earth. Ultimately, Newton determined mathematical equations that captured the nature of gravity and motion thereby providing a solid physical basis for Kepler's laws. The gravitational attraction (F) between two massive bodies is proportional to both masses (m_1 and m_2) and inversely proportional to the square of the distance (r) between them, or:

$$F = \frac{Gm_1m_2}{r^2}$$

The constant term, G, is known as the universal gravitational constant.

Gravity, the dominant long distance force in the universe, is sufficient to explain how the solar system stays together and many interesting phenomena that have been discovered. Some of the dynamic effects of gravity in the solar system are:

- Tides. Tides are the result of a difference in gravitational attraction to an object experienced at different locations. The most obvious manifestation of tides are the twice-daily fluctuations in the Earth's oceans. Caused by the combined forces of Moon and Sun, the Earth's oceans exhibit a bulge on the Moon-ward and far sides of Earth. On the Moon there's a matching bulge in the solid rock. Tidal effects exist throughout the solar system.

- Spin-orbit Coupling. A coupling between an object's spin and its orbit is a side effect of tides. Over time, tide induced torques will cause orbiting objects to slowly change their axial rotation. The change in rotation tends toward keeping a single side, usually the most massive side, permanently facing the orbited object[1]; rotating once for each orbit. Spin-orbit coupling is prevalent in the solar system, with all but a few major satellites exhibiting tidally locked rotation [7, p. 9].

- Orbit-orbit Resonance. Orbit-orbit resonances, or mean motion resonances, arise when two (or more) bodies orbit another so that the ratio of their orbital periods are close to an integer ratio. Symbolically: $T_1 : T_2 = p_1 : p_2$ where p_1 and p_2 are integers. The periodic alignments of these objects provide repeated disturbances that can have marked effects on long term orbits. Such arrangements are found throughout the solar system particularly between Jupiter and the asteroid belt, and amongst the satellites and rings of the Jovian planets.

- Orbital Precession. The presence of aspherical bodies and external forces from other orbiting bodies causes the slow rotation of elliptical orbit orientation over periods $\approx 10^5$ years: orbital precession. The most notable precession in the solar system is that of Mercury which was explained, at least to a reasonable approximation, by Newton's laws. A better approximation required Einstein's General Theory of Relativity which took several hundred years to come along.

Newton's formulation of gravity provided straightforward analytical answers in the case of two bodies free to move under the influence of gravity. It did not, however, take long to realise that solving the equations of motion for more than two bodies was difficult and, for the most part, impossible. In these systems each object is acted on by forces from every other object and,

[1] Actually facing the empty focus in the orbit, but the near-circular nature of the bulk of orbits makes this a fine distinction.

as the object moves, these forces change direction and magnitude. Many famous mathematicians have tackled what has come to be known as the N-body Problem and its relative the Three-body problem: Euler, Lagrange, Laplace, Jacobi, Le Verrier, Hamilton, Poincaré and Birkhoff [7, 6]. There remains no general analytical solution to this problem although interesting results, such as a figure-eight orbit by Chenciner and Montgomery [2], are announced from time-to-time.

Numerical Simulation

Given the intractable nature of the N-body problem the only practical method of analysing orbital motions for moderate or large N is by computer simulation. The general theme of numerical simulations is to convert the equations governing the dynamics of the system to a form suitable for calculation. For N-body simulations the equations must be converted to a discrete form that allows each successive set of object positions and velocities to be determined from the preceding set. These successive system states are usually separated by a small increment in time and the simulation process iterates over a multitude of these steps to determine the long term result. Modern digital computers are good at performing high volume numerical manipulations at high speed and are therefore well suited to this task.

Perhaps the most obvious approach to the N-body simulation is covered in many introductory courses on numerical methods. This approach requires only Newton's laws (in vector form) and basic physics to formulate.

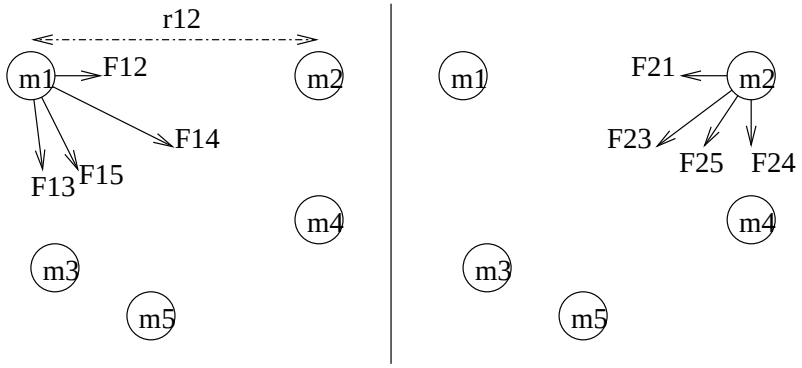

Figure 1: A typical multi-body situation. Object m1 is attracted towards each of the other objects which are, in turn, each attract to all the others. Each body will move under the influence of these constantly changing attractions.

Consider the situation depicted in Figure 1 in which particle m_1 is being attracted directly toward m_2 with force F_{12}, m_3 with force F_{13}, and so on. Direction is important in this situation so we need to use the vector form of

Newton's law[2]:

$$\mathbf{F} = \frac{Gm_1m_2}{|\mathbf{r}|^3}\mathbf{r}$$

The resultant force acting on particle m_1 from the other particles is:

$$\mathbf{F}_1 = \frac{Gm_1m_2}{|\mathbf{r}_{12}|^3}\mathbf{r}_{12} + \frac{Gm_1m_3}{|\mathbf{r}_{13}|^3}\mathbf{r}_{13} + \cdots + \tag{1}$$

Since the same summation needs to be applied to each particle in turn, we can write a more general form of Equation 1 for particle i:

$$\mathbf{F}_i = \sum_{j \neq i} \frac{Gm_im_j}{|\mathbf{r}_{ij}|^3}\mathbf{r}_{ij} \tag{2}$$

To convert this resultant force into motion Newton's third law of motion (Equation 3), which tells us that a force acting on a mass will cause an acceleration, is used. Solving for the acceleration and substituting Equation 2 for F leads to Equation 4.

$$\mathbf{F} = m\mathbf{a} \tag{3}$$

$$\begin{aligned} \mathbf{a}_i &= \mathbf{F}_i/m_i \\ &= \frac{1}{m_i}\sum_{j \neq i} \frac{Gm_im_j}{|\mathbf{r}_{ij}|^3}\mathbf{r}_{ij} \\ &= \sum_{j \neq i} \frac{Gm_j}{|\mathbf{r}_{ij}|^3}\mathbf{r}_{ij} \end{aligned} \tag{4}$$

The acceleration calculated at Equation 4 is the rate of change of velocity which we approximate with a straight line connecting two discrete velocity values:

$$\mathbf{a} = \frac{d\mathbf{v}}{dt} = \frac{\Delta\mathbf{v}}{\Delta t} = \frac{\mathbf{v}_{n+1} - \mathbf{v}_n}{\Delta t}$$

where subscripts n and $n+1$ indicate consecutive time steps. Rearranging we determine that:

$$\mathbf{v}_{n+1} = \mathbf{v}_n + \mathbf{a}\Delta t \tag{5}$$

Making the assumption that $\mathbf{v}$ is constant over the time increment Δt, and applying the same approximation for the rate of change, leads to the following position equation:

$$\mathbf{r}_{n+1} = \mathbf{r}_n + \mathbf{v}_n\Delta t \tag{6}$$

All the elements necessary to fill out the general sequence of events in simulation are now present. For each particle:

[2]The vector form is obtained by multiplying by a unit vector $\mathbf{r}/|\mathbf{r}|$ in the direction of the force.

- Calculate the resultant acceleration caused by all other particles (Equation 4).
- Determine the new velocity (Equation 5).
- Determine the new position (Equation 6.
- Plot or record the new data points, increment the simulation time by Δt and repeat.

Underlying the apparent simplicity of this approach outlined above are some disadvantages that make it unsuitable for large values of N. Chief amongst these is that the number of calculations required in each iteration is $O(N^2)$. For a simulation of the known solar system objects N approaches 100,000 and the load becomes unworkable. The amount of calculation required can be reduced by:

- Scaling masses, velocities and positions so that the constant G or some other element is eliminated.
- Assuming the objects are coplanar thereby removing one coordinate axis.
- Assuming that distant objects have little effect or can be more roughly approximated; a hierarchical approach.
- Calculating the motions at the vertices of a grid then applying these figures, or interpolated values, to all objects in the same grid square; a grid approach.
- Using a hybrid of the hierarchical and grid methods.

The grid and hierarchical approaches are often used with a more complex mathematical model of gravity. Some models treat gravity as a potential field (Poisson equation) and distribution of mass as a density function. Models may make use of Hamiltonian dynamics which simplifies the study of some motions at the cost of restrictions on math that may be used in unison. For example, Hamiltonian systems maintain a number of invariant characteristics that can be destroyed by direct integration methods. Symplectic integration methods are specially designed to support simulations using Hamiltonian dynamics.

In any numerical simulation accuracy and stability must be carefully guarded. In the accuracy of the direct summation described above, in which errors are accumulated over time, is governed by the size of the time interval (Δt) and the assumption of constant velocity during the interval. Figure 2 shows a simplified example of a small object dropped vertically to Earth (constant acceleration) with two discrete approximations. Clearly

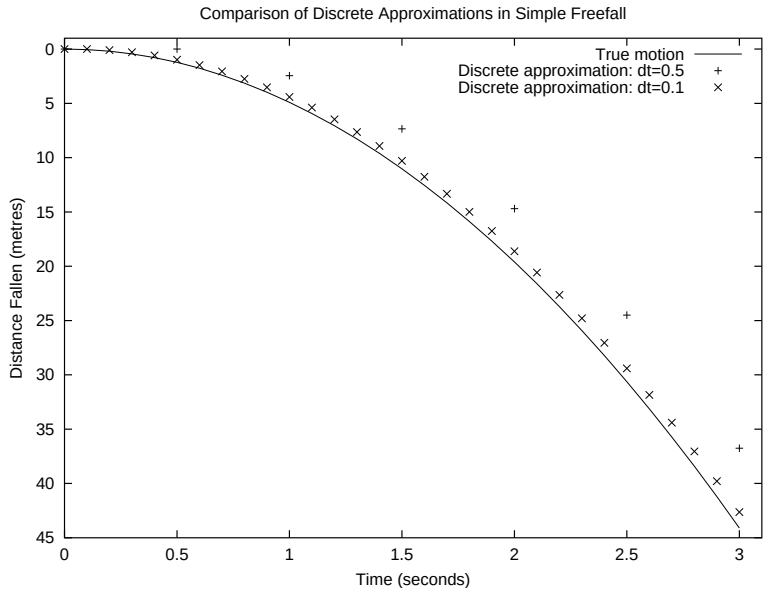

Figure 2: Difference between true motion and discrete approximations (0.5 and 0.1 second increments) for a small object dropped vertically to Earth (constant acceleration). Clearly the smaller time increment furnishes the better approximation.

the smaller time increment figure gives a better approximation of the true motion but comes at the cost of more calculation. Varying the time step as distance between objects decreases is one possible enhancement to the simulation. Δt variation need not be global, the bodies that are close can have several iterations at smaller increments applied between steps in the global simulation. For these extra iterations the forces caused by distant bodies are assumed fixed and only the motion of the close bodies are considered. Alternatively, a better approximation may be made by assuming constant acceleration over each time interval:

$$\mathbf{r}_{n+1} = \mathbf{r}_n + \mathbf{v}_n \Delta t + \frac{\mathbf{a}\Delta t^2}{2}$$

Other methods, that don't rely on smaller time increments, have been devised to improve accuracy. Predictor-corrector methods are one such scheme that uses the weighted (h, often 1) average of more than one estimated value to derive the next. Expressed in terms of the example simulation, $\mathbf{r}_n$ and $\mathbf{v}_n$ are used to determine a predicted position and velocity for the particle:

$$\begin{aligned} \mathbf{v}_{pred} &= \mathbf{v}_n + \mathbf{a}_n \Delta t \\ \mathbf{r}_{pred} &= \mathbf{r}_n + \mathbf{v}_n \Delta t \end{aligned}$$

The acceleration at the predicted position is also calculated. The new position and velocity, $\mathbf{r}_{n+1}$ and $\mathbf{v}_{n+1}$, are calculated:

$$\begin{aligned} \mathbf{v}_{n+1} &= \mathbf{v}_n + \frac{h}{2}(\mathbf{a}_n \Delta t + \mathbf{a}_{pred} \Delta t) \\ \mathbf{r}_{n+1} &= \mathbf{r}_n + \frac{h}{2}(\mathbf{v}_n \Delta t + \mathbf{v}_{pred} \Delta t) \end{aligned}$$

In the example of Figure 2 this scheme will determine a series of points on the ideal curve. While there is extra calculation involved in making and evaluating predictions, the extra load must be compared to the effect of decreasing the time increment to achieve the same accuracy.

The ability of the processing system to handle the required mathematical precision is also a factor in overall accuracy. In the calculations outlined earlier the system fails as $|\mathbf{r}|$ approaches zero, with F approaching infinity. Often a small factor is added to the denominator of Equation 4 ($|\mathbf{r}_{ij}|^3 + \epsilon$) to ensure that it does not become zero. For extreme distances the gravitational force will be extremely small which may result in numeric underflow and loss of precision problems.

Experimental Aims

One of the tasks assigned to the Swinburne University Supercomputer Facility is the simulation of dynamic systems including N-Body systems such as the solar system. For this project a simulation has been made available through a WWW based interface. The simulator's main characteristics are:

- All orbits are coplanar, major axes collinear, and perihelion occurs on the same side of the Sun (to the right in the plots).
- Initial planet positions alternate left to right of Sun, with the first on the left.
- A 2nd order predictor-corrector integration system[5].
- Scaled masses and distances.
- Up to nine planets with default parameters for the solar system.
- Simulation accuracy and period determined by the interplay of two parameters. The desired number of steps required to show the innermost orbit in the solar system is used to set the time increment: larger inner step counts correspond to small time increments. The total number of steps to run the simulation for determines the total running time.

The broad aim of the experimental part of the project is to use the provided simulation to explore the dynamics of the solar system. In particular,

the possibility of creating an unstable planetary system is to be investigated. Of the gravitational effects in multi-body systems (that the simulation can handle), resonant orbits and close approaches provide the most likely sources of physical instability. The choice of simulation parameters may lead to instability or inaccuracy that's not part of the physical system; this is also to be addressed.

There are three parts to the investigation:

- Show the effect of different time increment on the accuracy of the plotted orbits in the absence of large gravitational perturbations. These simulations will be used to select simulation parameters for the resonance and close approach experiments, and determine a baseline measure of the approximation error.
- Show the effects of resonance in the asteroid belt, using a (1) Ceres sized object, placed at and around the 2:1 Jupiter resonance distance. These simulations are expected to show the presence of physically unstable orbits in the asteroid belt region.
- Show the effects of a close pass of Jupiter by the same asteroid at subtly different pericentre distances, and with different simulation parameters. This is expected to highlight sensitive dependence on initial conditions and deleterious effects of poor numerical simulation parameters on systems with such sensitivities.

Results

To demonstrate the importance of the time increment in simulation accuracy, and determine a baseline accuracy, two basic runs were completed. Each simulation includes only two asteroids as detailed in Table 1, with one of the asteroids standing in for Jupiter and the other being set up at the 2:1 Jupiter resonance distance. These initial settings have been chosen to minimise gravitation interaction between the bodies leaving mainly numerical approximation errors. Run 1 (Figure 3(a)), with 100 steps to approximate the orbit of the inner asteroid (red) shows a markedly less defined orbit than Run 2 (Figure 3(b)) with 500 (maximum allowed). While the high resolution run does show a slightly less than perfect elliptical orbit for the inner asteroid, the orbit for the de-facto Jupiter (green) is tightly contained and well shaped. In contrast, the low resolution run's determination of the de-facto Jupiter's orbit wanders and is uneven.

The following resonance experiments will concentrate on the inner asteroid with a Jupiter of realistic mass in place. Any behaviour exhibited by the simulated asteroid could be the result of either approximation errors or real physical effects. If these numerical experiments were done with the lower inner orbit steps value they would be seriously affected by approximation

error. Consequently, the resonance experiments will be run at maximum resolution with the baseline error being that shown in Run 2.

Orbital resonance in the asteroid belt was explored with a series of five simulations with the parameters shown in Table 1 as Runs 3 to 7. The orbit of Run 3 lies in the Kirkwood gap where the orbital period is half that of Jupiter. The 2:1 resonant orbital distance, 3.278 AU, was calculated using the formula:

$$a_{Asteroid} = a_{Jupiter} / \sqrt[3]{4}$$

which is directly derived from Kepler's third law. The other orbits, either side of the resonant distance, were spaced at 0.075 AU increments. The results are shown in Figures 4 to 8 with Jupiter appearing in green and the asteroid in red.

Figure 4 is the result for an object placed in an orbit with a period half that of Jupiter. The orbit of the asteroid very quickly deviates from the initial near-circular state so that aphelion is driven as high as 3.7 AU and perihelion as low as 2.75 AU. The average orbital distance seems to have changed because the eccentricity required for the new perihelion (e=0.161) would result in a slightly higher than observed aphelion. The maximum aphelion and minimum perihelion are collinear with the Sun, consistent with belonging to the same orbit. Assuming the same orbit then the average distance, eccentricity, and orientation have changed to a=3.225 and e=0.147. The alignment of of maxima and minima may, however, be an artifact of over-plotting many varied orbits. Unfortunately, limited access to output data means it's difficult to determine if the maxima and minima belong to the current orbit, or if the evolution of the orbit has stabilised. Clearly though, the simulation shows that an asteroid orbit at the 2:1 resonance distance is not stable.

The simulation assigned initial position for the asteroid is at aphelion in superior conjunction with Jupiter. The first conjunction occurs one asteroid orbit later with the asteroid and Jupiter at aphelion. Murray and Dermott [7, Chapter 8] indicates that such an arrangement is unstable. If perfectly aligned then there's no net tangential force acting on the asteroid as it passes conjunction. However, if the alignment is even slightly asymmetric then a net tangential force acts on the asteroid. The force acts to increase or decrease the asteroid's angular momentum and mean motion with the result that subsequent conjunctions are closer to perihelion. Once conjunctions are occurring at perihelion there's no longer a net tangential force. The asteroid will continue to experience a radial force at each conjunction causing a delay in reaching perihelion. The asteroid orbit will precess in the prograde sense[3].

Inward in steps of 0.075 AU from the resonant distance are the progressively more contained orbits of Figures 5 and 6. The innermost orbit,

[3]Precession also results from orbiting an oblate object, like the Sun, but this effect is not modeled by this simulation.

at 3.128 AU, is confined to a narrow region although it is still perturbed by Jupiter (compare to Run 2 Figure 3(b)). This region coincides with a marked concentration of asteroids in the asteroid belt around the orbit of (24) Themis at 3.137 AU.

Movement in 0.075 AU steps outward from the 2:1 resonance distance also leads to orbits less spread than at resonance. The improvement is less marked than the change for inward movement. Figure 7 is only marginally less spread than at resonance while Figure 8 is less contained than the equivalent distance inside the resonant orbit. The outer distance corresponds to a small peak in asteroid numbers in the region of (65) Cybele at 3.432 AU [1, Ch 25. Asteroids].

Six simulation runs were made to explore the effects of close approaches to the orbit of Jupiter. The parameters are shown in Table 1 as Runs 8 through 11. The simulations were run in pairs over a long (Runs 8, 10, 12) and short (Runs 9, 11, 13) period to allow comparison of overall evolution and the early source of variation. The orbit semi-major axis was chosen so that it had no particular resonant relationship to Jupiter's orbit and a reasonable eccentricity would bring it close to Jupiter's orbit. At least on the first orbit, Jupiter would not come as close as these figures would indicate because of initial starting position on opposite sides of the Sun.

Figures 9(a) and 9(b) show the simulation over long and short periods of an orbit that passes within 0.25 AU of Jupiter's at aphelion. The long term trajectory of the asteroid varies quite dramatically from as low as 1.8 AU out to the orbit of Uranus. The plot of the first orbits shows that several orbits are completed close to the starting distance, but on the third orbit the asteroid is drawn into two close encounters with Jupiter that propel into an orbit not far outside Jupiter's. Several orbits later the asteroid is ejected further into the outer solar system. In general, each orbit seems to be travelled several times before making a substantial change as a result of interaction with Jupiter. Examination of the orbit at such times might give the impression that the orbit was stable. Such a pattern is often a characteristic of chaotic systems although it does not necessarily mean that a system is chaotic.

A slightly closer approach (0.24 AU) is shown for long and short durations in Figures 10(a) and 10(b) respectively. The small change in proximity to Jupiter's orbit, roughly 4 times the Earth-Moon distance, has substantially altered the short and long term evolution of the system. Excursions into the outer solar system do not go as far as in the previous case. The pattern of repeated traversals of similar orbits continues, with each outer loop containing several passes. The short duration simulation of the seminal orbits show that quite large differences between Figure 10(b) to Figure 9(b) appear very early in the simulation. High sensitivity to initial conditions is a trait associated with chaotic systems.

To confirm the chaotic, or closed periodic, nature of these orbits would

require further analysis of the data output from the simulation. One method that could be employed to depict the stability of the system is a phase space plot. A plot of x versus $\dot{x}$ for $y = 0$ and $\dot{y} > 0$ will show a closed curve, or curves, for regular orbits while a chaotic orbit will show scattered dots that, over time, fill a volume.

Figures 9(a) and 10(a) show that the orbit of Jupiter is mildly distorted from the crisp single line expected of the simulation. The accumulation of small errors of a long simulation may be producing this spreading of the orbit. To further investigate the effect of simulation parameters the earlier close approach simulation for 0.25 AU (Runs 8 and 9) was re-run with a very slightly smaller number of steps for the inner-most orbit i.e. a slightly larger Δt. The results, at Figures 11(a) and 11(b), show a dramatically different path over time and that the changes started very early in the simulation. The change of number of inner orbit steps from 500 to 499 has changed the entire simulated evolution. Clearly, simulation errors can become a substantial issue when attempting to simulate phenomena that have chaotic or sensitive regimes.

This result casts doubt over the accuracy of the simulations in Runs 8 through 11. It's no longer clear whether the displayed behaviour is the result of the physical system behaviour or numerical approximation and errors. Indeed, only general characteristics seem to be trustworthy: close approach to Jupiter can cause wild variation in trajectories of the asteroid. Re-running the resonance experiments, Runs 3 through 7, with the smaller inner orbit step count (499) shows no appreciable differences in gross properties allowing a much higher degree of confidence that the behaviour is physical.

Conclusions

The insights of Kepler and Newton provided a basis for the understanding of dynamics in the solar system and further afield. The problem of determining the behaviour of many objects free to move under the influence of gravity has proven to be a difficult mathematical challenge. Since the advent of the general purpose computer the numerical simulation of such systems has become possible. Simulations can cover the full range of gravitational phenomena from orbit determination to simulation of large scale structures in the Universe.

Simulation of the motion of a small body at the 2:1 Jupiter resonance shows that such an orbit is quickly altered. However, simulated orbits slightly either side of the mean motion resonance are more stable. The result does not seem to be extremely sensitive to simulation parameter choices and can confidently be treated as close to the physical behaviour. Indeed, the more stable orbits are mirrored in the asteroid belt by concentrations of asteroids around (24) Themis and (65) Cybele, while the absence of asteroids

at the resonance point is marked.

Proximity to Jupiter can be quite dramatic for a small body. Close approaches can to alter the orbit in ways that range from subtle to dramatic, sometimes sending the object far out in the solar system. The simulation shows a sensitive dependence on the initial conditions, both physical and numerical, for close encounters with small changes making dramatic difference to the long term trajectory of the small body. Further, the trajectories seem to have varying periods of stability between dramatic alterations of course. Both sensitivity to initial conditions and erratic changes in the system are traits of chaotic systems.

The accuracy and stability of the simulation algorithms themselves must be considered when using numerical methods. Making unsuitable approximations, choosing parameters poorly, or limitations of the calculating machinery can all play a part in the accuracy of simulation. The effects of simulation errors may be small in comparison to the key phenomena but, in a potentially chaotic system, small input differences can make large changes in long term behaviour. The effects of accumulating simulation differences are amply shown in the simulation (Runs 1, 12 and 13) used for this project.

Simulation is a powerful tool to aid in the understanding of the dynamics of objects in the solar system. Provided the numerical model is well constructed, and parameters well chosen, it may be used to extrapolate both forward and back in time to see our solar system evolve.

References

[1] J. Kelly Beatty, Carolyn Collins Peterson, and Andrew Chaikin, editors. *The New Solar System*. Cambridge University Press, 4th edition, 1999.

[2] Alain Chenciner and Richard Montgomery. A remarkable periodic solution of the three body problem in the case of equal masses. *Annals of Mathematics*, 152(3):881–901, 2000.

[3] Amara Grap. Amara's recap of particle simulation methods. Internet `http://www.amara.com/papers/nbody.html`, March 2000.

[4] Sarah Maddison. Tools of Modern Astronomy: Numerical Simulations. HET606 Course Material, Swinburne University of Technology, 2000.

[5] Sarah Maddison. Re: writing a dynamics simulator. Newsgroup posting (subjects.hetxxx.projects01s2), 2 November 2001.

[6] C. Marchal. *The Three-Body Problem*. Elsevier, Amsterdam, 1990.

[7] Carl D. Murray and Stanley F. Dermott. *Solar System Dynamics*. Cambridge University Press, 1999.

[8] Ettore Perozzi. Resonance. In *Encyclopedia of Astronomy and Astrophysics*. Nature Publishing Group, 2001.

Run	Object	Mass (M_{Earth})	Semi-major Axis (AU)	Eccentricity	No. of Steps	Inner Orbit Steps	Description
1	Asteroid	0.0001	3.278	0.048	10000	100	Asteroids, one standing in for Jupiter, 100
	Asteroid	0.0001	5.203	0.048			inner orbit steps
2	Asteroid	0.0001	3.278	0.048	50000	500	Asteroids, one standing in for Jupiter, 500
	Asteroid	0.0001	5.203	0.048			inner orbit steps
3	Asteroid	0.0001	3.278	0.048	100000	500	2:1 resonance, Kirkwood gap
4	Asteroid	0.0001	3.203	0.048	100000	500	Slightly inside 2:1 resonance
5	Asteroid	0.0001	3.128	0.048	100000	500	Further inside 2:1 resonance
6	Asteroid	0.0001	3.353	0.048	100000	500	Slightly outside 2:1 resonance
7	Asteroid	0.0001	3.428	0.048	100000	500	Further outside 2:1 resonance
3-7	Jupiter	317.83	5.203	0.048			
8	Asteroid	0.0001	4.336	0.200	100000	500	Close approach (0.25 AU) at aphelion
9	Asteroid	0.0001	4.336	0.200	2000	500	Close approach, first orbits
10	Asteroid	0.0001	4.336	0.202	100000	500	Close approach (0.24 AU) at aphelion
11	Asteroid	0.0001	4.336	0.202	2000	500	Close approach, first orbits
12	Asteroid	0.0001	4.336	0.200	100000	499	Close approach (0.25 AU), lower resolution
13	Asteroid	0.0001	4.336	0.200	2000	499	Close approach, lower resolution, first orbits
8-13	Jupiter	317.83	5.203	0.048			

Table 1: Simulation run parameters.

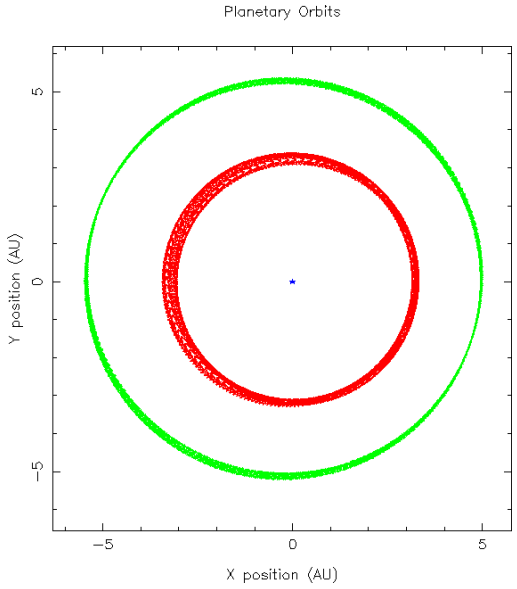

(a) Run 1. Low resolution, 10000 steps at 100 steps per inner orbit

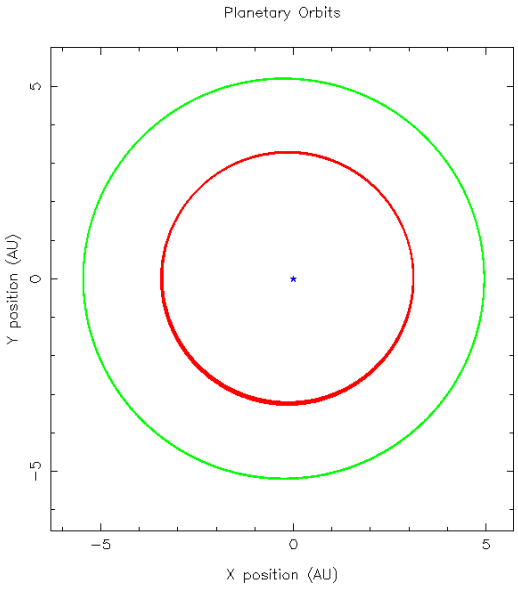

(b) Run 2. High resolution, 50000 steps at 500 steps per inner orbit

Figure 3: Two asteroids. One asteroid is standing in for Jupiter while the other is set up as for the resonance experiments that follow. The small masses minimise gravitational perturbation leaving mainly numerical inaccuracies.

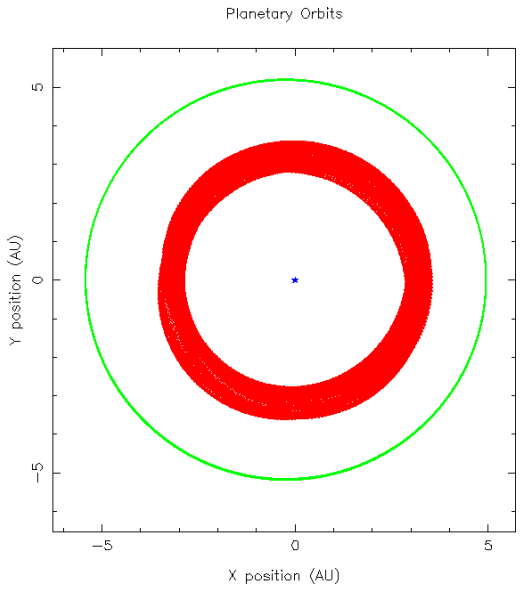

Figure 4: Run 3. Asteroid at 2:1 orbital resonance with Jupiter. Starting orbital distance is 3.278 AU, with mass of 0.0001 and eccentricity 0.048. This region is called the Kirkwood Gap.

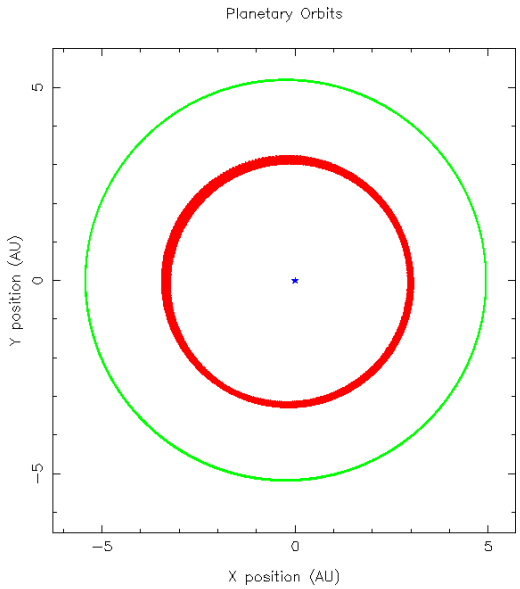

Figure 5: Run 4. Asteroid 0.075 AU inside the 2:1 resonant orbit with Jupiter.

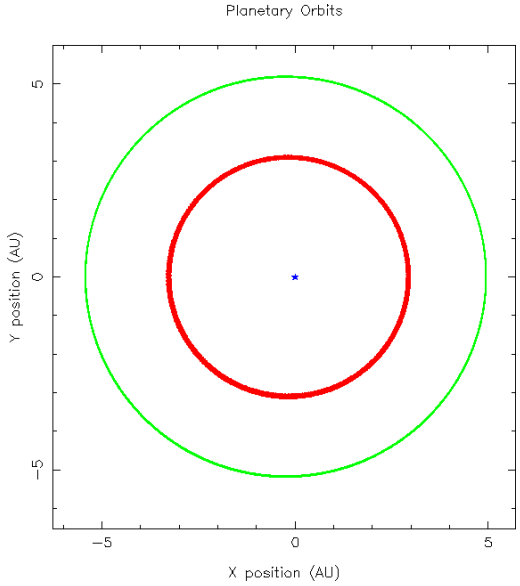

Figure 6: Run 5. Asteroid 0.15 AU inside the 2:1 resonant orbit with Jupiter. This orbit corresponds with a large concentration of asteroids around (24) Themis.

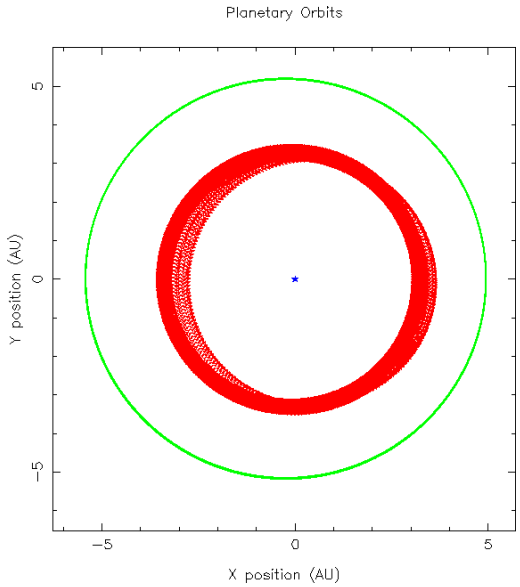

Figure 7: Run 6. Asteroid 0.075 AU outside the 2:1 resonant orbit with Jupiter.

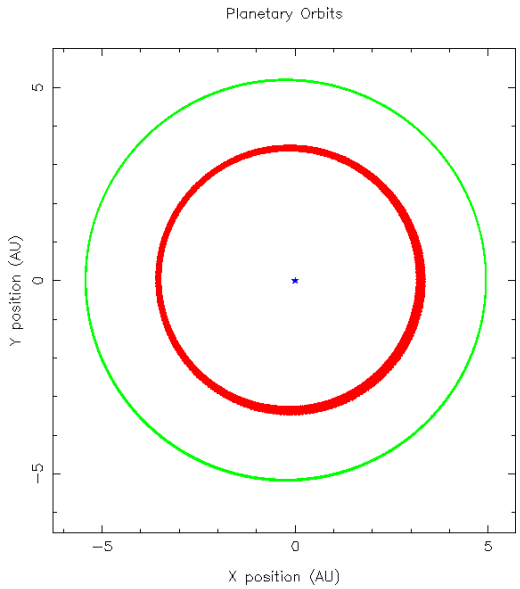

Figure 8: Run 7. Asteroid 0.15 AU outside the 2:1 resonant orbit with Jupiter. This orbit corresponds with a small concentration of asteroids around (65) Cybele.

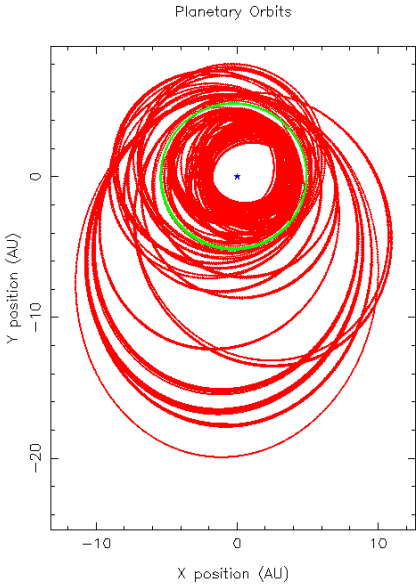

(a) Run 8. Long term simulation

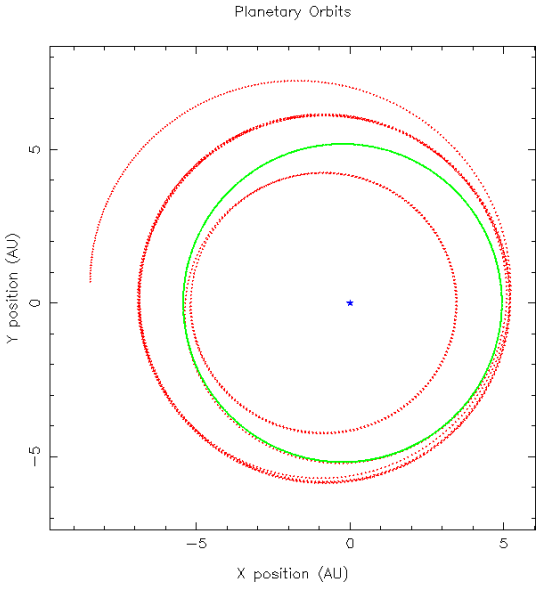

(b) Run 9. Short term simulation

Figure 9: Runs 8 and 9. Asteroid with average distance of 4.336 AU, eccentricity 0.2. The orbit approaches to within 0.25 AU of Jupiter's orbit at aphelion.

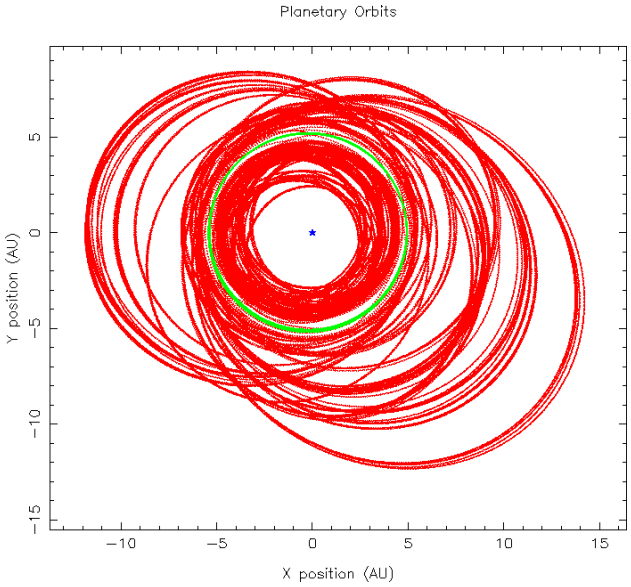

(a) Run 10. Long term simulation

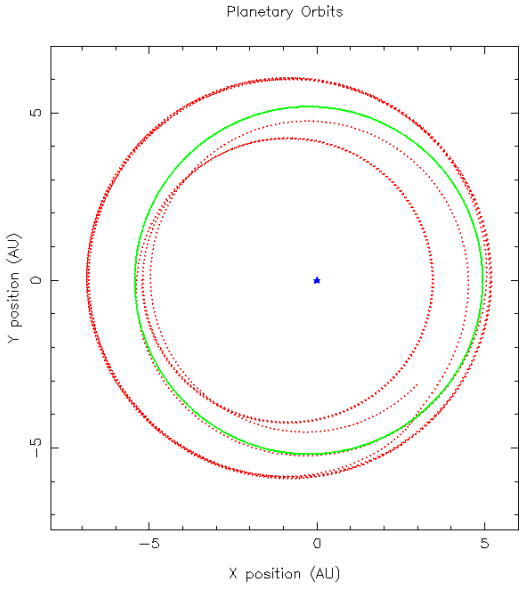

(b) Run 11. Short term simulation

Figure 10: Runs 10 and 11. Asteroid with average distance of 4.336 AU, eccentricity 0.202. The orbit approaches to within 0.24 AU of Jupiter's orbit at aphelion.

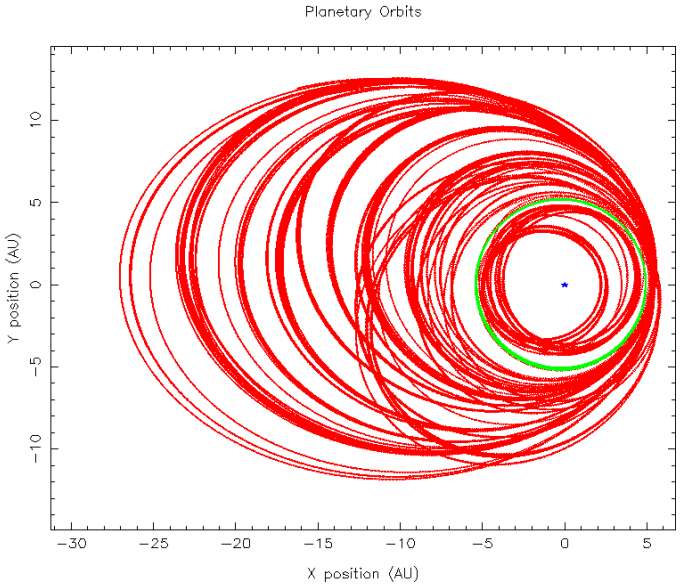

(a) Run 12. Long term simulation

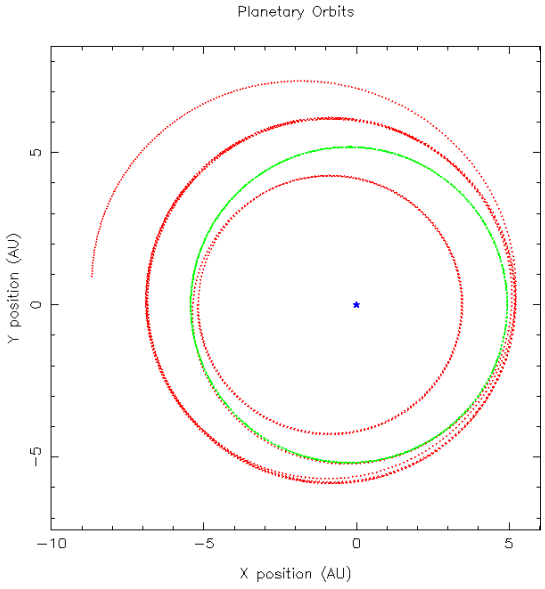

(b) Run 13. Short term simulation

Figure 11: Runs 12 and 13. Asteroid with average distance of 4.336 AU, eccentricity 0.2 simulated at lower resolution than Run 8. The long term trajectory is significantly different.